Journal of Nanoscience and Nanotechnology

Tunable cytotoxicity and selectivity of phosphonium ionic liquid with aniline blue dye

Samantha Macchi[1], Mohd Zubair[2], Nawab Ali,[2] Grégory Guisbiers[3], and Noureen Siraj[1,*]

[1]*Department of Chemistry, University of Arkansas at Little Rock, 2801 S. University Ave, Little Rock, AR 72204, USA*

[2]*Department of Biology, University of Arkansas at Little Rock, 2801 S. University Ave, Little Rock, AR 72204, USA.*

[3]*Department of Physics and Astronomy, University of Arkansas at Little Rock, 2801 S. University Ave, Little Rock, AR 72204, USA.*

*Corresponding author: Noureen Siraj, Email: nxsiraj@ualr.edu

Author - Please insert Dates here for the accepted final manuscript.

Submitted/Received: ……..……. Revised/Accepted: ……..……

Abstract

Ionic liquids are an interesting class of materials that have recently been utilized as chemotherapeutic agents in cancer therapy. Aniline blue, a commonly used biological staining agent, was used as a counter ion to trihexyltetradecylphosphonium, a known cytotoxic cation. A facile, single step ion exchange reaction was performed to synthesize a fluorescent ionic liquid, trihexyltetradecylphosphonium aniline blue. Aqueous nanoparticles of this hydrophobic ionic liquid were prepared using reprecipitation method. The newly synthesized ionic liquid and subsequent nanoparticles were characterized using various spectroscopic techniques. Transmission electron microscopy and zeta potential measurements were performed to characterize the nanoparticles' morphology and surface charge. The photophysical properties of the nanoparticles and the parent aniline blue compound were studied using absorption and fluorescence spectroscopy. Cell viability studies were conducted to investigate the cytotoxicity of the newly developed trihexyltetradecylphosphonium aniline blue nanoparticles in human breast epithelial cancer cell line (MCF-7) and its corresponding normal epithelial cell line (MCF-10A) in vitro. The results revealed that the synthesized ionic nanomedicines were more cytotoxic (lower IC_{50}) than the parent chemotherapeutic compound in MCF-7 cells. Nanoparticles of the synthesized ionic liquid were also shown to be more stable in both aqueous and cellular media and more selective than parent compounds towards cancer cells.

Keywords: ionic liquids, nanoparticles, cytotoxicity, reprecipitation

1. Introduction

Cancer remains one of the leading causes of death worldwide, surpassed only by heart disease. Breast cancer is one of the most common cancers diagnosed, especially amongst women, with about 1 in 8 women developing an invasive form over the course of their life [1]. Many different therapies for the treatment of cancer have been explored and utilized. However, most of these methods including chemotherapy and radiation therapy have significant adverse side effects associated with them [2, 3]. This has prompted researchers to investigate new ways of treating various cancers with reduced harm to the patient. An important aspect of this goal is the design and synthesis of drugs that can easily and accurately target tumor cells. One way to accomplish the selectivity of drugs towards cancer cells is to implement nano-scale drug design.

The field of nanotechnology encompasses many scientific disciplines and most simply refers to the design and utilization of materials having at least one dimension less than roughly 500 nanometers (nm) [4]. Nanotechnology applications have grown significantly within the field of pharmaceutical research in recent years due to the potential advancement in drug design [5–7]. Nano-scale drugs offer several advantages to the traditional counterparts as they offer much more efficient and safer delivery to tissues [8, 9]. Recently, nanodrugs have also shown preferential uptake in tumors due to the enhanced permeability and retention (EPR) effect [10]. In the last ten years, the most common application of nanomaterials in the industry is the use of nanoparticles (NPs) as drug delivery devices [11–14]. This approach, while it optimizes delivery and reduces side effects, adds an additional and oftentimes complicated step to synthesis with its own safety concerns. Thus, development of carrier-free NP-based drugs can prove to be more economical in terms of synthesis and delivery to tissues [15].

Ionic liquids (ILs) are a rapidly growing and exciting class of materials with potential for many applications. ILs are defined as organic salts that have much lower melting points (below 100 ^{o}C) than traditional ionic compounds. ILs possess a unique set of characteristics such as low volatility and vapor pressure, high thermal stability, and very good solvent properties for a variety of compounds [16, 17]. These materials are also highly tunable and have been recently sought out for use in pharmaceutical applications [18, 19]. Many commonly used ILs, such as alkyl substituted ammonium and phosphonium-based ILs, are studied in terms of their toxicity in many cell lines with varying IC_{50} values are reported [20–22]. The toxicity of these kinds of cationic ILs is highly dependent on their lipophilic nature [23, 24]. The ammonium and phosphonium-based ILs are colorless, thus they do not absorb or fluoresce visible light. Therefore, their cellular uptake mechanism and localization remains unknown. However, replacing a non-cytotoxic counterion (chloride, etc.) in these compounds with a non-toxic fluorescent ion can help to investigate the subcellular localization of the compounds, and the cell death mechanism can easily be tracked. Moreover, these ILs can form aqueous nanostructures (micelles, NPs, etc.) depending on their

noncovalent interactions [25] and alkyl chain length [26]. By altering these interactions (hydrogen bonding, hydrophobic, and pi-pi stacking) the nanostructures can be strategically tuned [27].

Herein, we have designed and synthesized a tandem fluorescent/chemotherapeutic IL using a rapid, cost-effective, metathesis reaction. Aniline blue, a common non-toxic staining dye, was used as the fluorescent moiety while trihexyltetradecyl phosphonium IL was used as a cytotoxic ion. The cytotoxicity of trihexyltetradecyl phosphonium is established in cancer cells with various anions such as bis[(trifluoromethyl)sulfonyl]amide [NTF_2] [22] and ampicillin [Amp] [28]. The resultant hydrophobic product was characterized using different spectroscopic techniques including UV-Visible and fluorescence spectroscopy. NPs were prepared from the hydrophobic IL via precipitation method in aqueous and cell media. The photophysical characterization of these carrier-free NPs was then performed. The application for these NPs as nanomedicines was investigated in terms of their size, morphology, surface charge, and cytotoxicity in cancerous and non-cancerous model cell lines.

2. Experimental Details

2.1. Materials

Sodium aniline blue (Na_2AB) was purchased from Allied Chemical Corporation (Morristown, NJ). Trihexyltetradecylphosphonium chloride (TTPCl) and deuterated (d-6) dimethyl sulfoxide (DMSO) were purchased from Sigma-Aldrich (Milwaukee, WI). Distilled deionized water (18.2 MΩ cm) was obtained using Purelab Ultrapure water purification system (ELGA, Woodridge, IL) and used to prepare nanomaterials. Cell culture grade DMSO, dichloromethane (DCM) and ethanol were purchased from VWR (Radnor, PA). Spectrosil® quartz cuvettes (Starna, Atascadero, CA) were used for all spectrophotometric measurements. Lacey carbon Transmission electron microscopy (TEM) grids with 200-mesh copper were purchased from Ted Pella (Redding, CA) to characterize NP size. MCF-7 and MCF-10A cell were obtained from American Type Culture Collection (ATCC, Manassas, VA). Dulbecco's Modified Eagle's Medium, Trypsin-EDTA 0.25%, Penicillin, Streptomycin and Minimal Essential Medium were purchased from Caisson Lab (Smithfield, UT). Fetal bovine serum (FBS) was obtained from Atlanta Biologicals (Lawrenceville, GA). Mammary Epithelial Cell Basal Medium with supplement pack (epidermal growth factor, insulin, hydrocortisone, and bovine pituitary extract), gentamicin, and amphotericin B were purchased from PromoCell (Heidelberg, Germany). Phosphate Buffered Saline (PBS), pH 7.4 and trypan blue, solution were purchased from Fisher Scientific (Waltham, MA).

2.2. ILs and NPs synthesis

Na_2AB and TTPCl were dissolved in DCM in a molar ratio of 1:2 and stirred until complete solvation. In order to remove small hydrophilic counterions (Na^+, Cl^-), deionized (DI) water was added to the solution and it was again stirred for approximately 24 h (Figure 1). The water layer containing sodium and chloride ion was removed. The organic layer was washed five times to

completely remove the sodium chloride by-product. The complete removal of sodium chloride was ensured by performing a precipitation testing of chloride using silver nitrate. The resultant organic layer was rotary evaporated until dry. The new IL was collected and named $[TTP]_2[AB]$. The resultant material was a highly hydrophobic product that was deep blue in color.

NPs of the hydrophobic $[TTP]_2[AB]$ IL were prepared via simple reprecipitation method in water. Briefly, a few microliters of concentrated solution (1 mM) of IL in ethanol was dropwise added to a scintillation vial of deionized water in an active sonication bath (Cole Palmer, 40 kHz). The vial was allowed to sonicate for five minutes with a thirty-minute rest period prior to measurements.

2.3. Physical Characterization

Electrospray ionization tandem Mass Spectrometry (ESI-MS) was performed using an Agilent (Santa Clara, CA) 1100 Series LC/MSD Trap VL to characterize the newly developed trihexyltetradecylphosphonium aniline blue $[TTP]_2[AB]$ IL. Nuclear magnetic resonance (NMR) was performed using JEOL 400 MHz instrument in deuterated DMSO. In order to characterize the morphology of NPs, TEM was performed with a JEM-2100F (JEOL, Tokyo, Japan), equipped with a Schottky field emission gun. NPs were prepared in water and 4 µL of the suspension was loaded onto a copper mesh TEM grid. Zeta potential measurements were taken using a Litesizer 500 (Anton Paar, Graz, Austria) Dynamic light scattering (DLS) particle size analyzer to investigate the surface charge and stability of the nanomaterials. DLS was performed with Malvern Panalytical (Malvern, United Kingdom) Zetasizer instrument using a 90-degree scatter angle. IL-based NPs were characterized in aqueous solvent for DLS and zeta potential measurements.

2.4. Photophysical Characterization

Photophysical properties of the parent compound (Na_2AB) and $[TTP]_2[AB]$ IL were analyzed via UV-Vis Spectroscopy. Compounds were analyzed photophysically in ethanol solvent and in water as NPs. A Cary 5000 UV-Vis-NIR (Agilent, Santa Clara, CA) double beam spectrometer was utilized for absorbance measurements. Fluorescence spectrophotometry was performed using polished 4-sided quartz cells and Horiba NanoLog spectrofluorometer (Kyoto, Japan).

2.5. Cell Culture/Sample Preparation

MCF-7 cells were maintained as a monolayer at 37 ^{o}C 5% CO_2 in Dulbecco's Modified Eagle's Medium (DMEM) supplemented with 10% (v/v) FBS, penicillin (500 units/mL) and streptomycin (500 units/ml). MCF-10A cells were maintained in Mammary Epithelial Cell Basal Medium supplemented with epidermal growth factor (10 ng/mL), insulin (5 µg/mL), hydrocortisone (0.5 µg/mL), bovine pituitary extract (0.004 mL/mL), gentamicin (100 µg/mL), and amphotericin B (0.05 µg/mL). At desired confluence, cells were sub-cultured by trypsinization and counting of the detached cells using a hemocytometer following staining with trypan blue exclusion dye. For experiments, cells were seeded at a density of 3×10^4 cells per well in a 96-well plate and grown for 24 h. The cells were then treated with varying doses of the drugs. Parent and

$[TTP]_2[AB]$ NPs were prepared at various concentrations by diluting stock solution in cell culture media following bath sonication while maintaining a sterile environment. DMSO concentration was at 0.5% to avoid any cellular toxicity. Cells were treated with different doses of drugs (0.5-10 μM) and incubated for 24 h in a humidified (5%) CO_2 incubator at 37 °C. Appropriate controls with complete media alone and vehicle control without NPs (DMSO) were included. Following incubation, medium was carefully aspirated, and cells were washed twice with PBS, pH 7.4. MTT assay was performed according to manufacturer's protocol and as described earlier [29] to assess cell viability. A Synergy H1 microplate reader (BioTek, Winooski, VT) was used to determine optical density at 570 nm for MTT assay. Statistical analysis was performed using two-tailed t-test against vehicle control. P values are denoted as: * $p<0.05$, ** $p<0.01$, *** $p<0.005$.

2.6. Cellular uptake

About 3×10^4 cells per well were seeded in a 96-well plate for 24 h at 37 °C. Following incubation, cells were treated with different concentration of NPs (0.5-10 μM) for 24 h. Appropriate controls with NPs resuspended in complete media alone and vehicle control without NPs (DMSO/DMEM) were included. Following incubation, cells were washed with PBS and replaced with fresh complete cell media. Fluorescence emission intensity was recorded using Cell Imaging Multimode Reader (Cytation 5, BioTek, Winooski, VT) at excitation and emission wavelengths of 300 nm and 355 nm, respectively.

3. Results and Discussion

3.1. Physical Characterization

Characterization of IL-Based Photosensitizer and NPs

The resulting IL was characterized using ESI-MS. The peak observed in mass spectra positive ion mode confirmed the TTP^+ cation (mass/charge ratio = 483.6; calculated ion mass = 483.86) and in negative ion mode mass peak confirms AB^{2-} anion (mass/charge ratio = 691.5; calculated ion mass = 691.74) in the synthesized IL, $[TTP]_2[AB]$. Proton NMR was performed to confirm the ratio of $[TTP]_2[AB]$. ^{1}H-NMR (d_6-DMSO, 400 MHz): 10.21(s, 1H), 7.18(m, 24H), 2.15(m, 16H), 1.36(m, 96H), 0.84(s, 24H). This data further confirms the identity of $[TTP]_2[AB]$ by revealing 2:1 TTP:AB ratio (136:25 protons, with 68 corresponding to one equivalent of TTP^+ and 25 to AB^{2-}). The melting point of $[TTP]_2[AB]$ was found to be 16 °C.

TEM images revealed that NPs of $[TTP]_2[AB]$ are cubical shaped with length of 49.6±10.9 nm (Figure 2). Na_2AB NPs are colloidally unstable and thus TEM was not feasible for this compound. To further confirm the stability of the NPs, zeta potential measurements were performed to acquire the surface charge of the nanomaterials. Greater magnitudes of zeta potential values can be related to the colloidal stability of the suspension. In general, a NP surface charge of at least ±30 mV can be considered electrostatically stable and can be considered sterically stable at ±20 mV [30]. These measurements can be utilized to gain insight into the interaction of NPs with cancerous and noncancerous cells [31]. The zeta Potential values for nanomaterials of the

parent photosensitizer, Na_2AB and $[TTP]_2[AB]$ were found to be -15 mV and +35 mV, respectively. Thus, the conversion of AB to an IL increases the magnitude of zeta potential in aqueous media and alters the surface charge to become a positive value. This is advantageous when combatting cancer cells, because cancer cells are slightly more negative on the surface than normal cells [32].

DLS measurements of NPs revealed a hydrodynamic diameter in water of 48.7±4.5 nm and 109.15±8.0 nm for Na_2AB and $[TTP]_2[AB]$, respectively. The hydrated sizes of the nanomaterials are typically larger in size as compared to the dried NPs due to the presence of solvent molecules. When NPs are prepared in cell media, hydrodynamic diameters are found to be 7.6±2.3 nm and 117.0±11.2 nm for Na_2AB and $[TTP]_2[AB]$, respectively.

Visual stability studies were also conducted by subjecting four different concentrations of suspensions of both Na_2AB and $[TTP]_2[AB]$ nanomaterials following settling of the materials in transparent tubes for 24 h in the dark. From Figure 3a. it is seen that the parent compound Na_2AB NPs show significant aggregation, with particles falling out of suspension after 24 h. The IL based NPs (Figure 3b.) show little to no aggregation, indicating the enhanced stability of these particles. Both types of NPs gave homogenous suspensions without any aggregations observed at all concentrations before settlement at time zero.

3.2. Photophysical Characterization

IL-based photosensitizer, $[TTP]_2[AB]$ and parent dye (Na_2AB) were examined in terms of their photophysical properties. Both parent compound and IL solution in ethanol exhibited three absorption peaks at ~300, 375, and 590 nm, and no shift in wavelength maxima was observed upon conversion to IL. The newly developed IL exhibits enhanced molar absorptivity at all three peak maxima in comparison to the parent Na_2AB compound in ethanol (Figure 4a). The difference in absorbance intensity can be attributed to inhibition of aggregation between AB anion in the presence of bulky TTP ions [33, 34].

Fluorescence emission spectra were recorded for both $[TTP]_2[AB]$ ILs and Na_2AB parent compound in ethanol solvent at an excitation wavelength of 290 nm. Fluorescence emission spectra for both compounds are identical in shape and Na_2AB fluorescence emission intensity is slightly greater than $[TTP]_2[AB]$ (Figure 4b). Thus, our results indicate that counterions affect the photophysical properties of the photosensitizer.

Absorbance spectrum of Na_2AB NPs is very similar in shape as compared to in ethanolic solution (Figure 5a). However, there is a significant reduction in absorption intensity at the major wavelength maxima, and this peak occurring at 595 nm is slightly blue shifted to 585 nm. This shift in absorbance spectrum to lower wavelength is attributed to the formation of face-to-face H-aggregates in the NP form of Na_2AB. The lowered molar absorptivity of Na_2AB is attributed to the agglomeration of NPs. Absorption spectrum of $[TTP]_2[AB]$ NP suspension in water shows a dramatic reduction in the absorption intensity at 590 nm peak as compared to their ethanolic solution spectrum, as well as an intense blue shift to 525 nm. This reduced absorbance intensity is

attributed to the presence of bulky phosphonium cations at the surface of NPs as indicated by the positive value of zeta potential. These colorless phosphonium ions do not absorb light and shield the photosensitizer dye from interaction with light in suspension. It should be noted that the NPs form of both the parent and IL compound are almost completely devoid of the peak at ~375 nm. Molar absorptivity values for ILs and parent dye in both ethanol and water are highlighted in Table 1.

[Insert Table 1]

Upon conversion of the compounds to nanomaterials in aqueous media, fluorescence emission intensity is significantly dropped. This is due to H-type dimer formation of both species in the nanoform which results in aggregation-induced emission quenching [35]. Fluorescence emission spectra for both Na_2AB and $[TTP]_2[AB]$ in water are shown in Figure 5b. Peak maximum of emission is red shifted for both compounds from 355 nm in solution to 375 nm and 410 nm for Na_2AB and $[TTP]_2[AB]$ NPs, respectively.

3.3. *In Vitro* Cytotoxicity Studies

In order to establish a potential application of the newly synthesized IL in cancer treatment, cell viability studies were performed on human breast cancer MCF-7 and their corresponding noncancerous MCF-10A cells. These cell lines were treated with various concentrations of the synthesized IL ($[TTP]_2[AB]$) and both parent compounds (TTPCl and Na_2AB) for 24 h. The cell viability was then determined following MTT assay in order to assess their chemotherapeutic ability. MTT assay is a widely used method to evaluate cytotoxicity of newly developed cancer treatment drugs in *vitro*. In this study, the parent Na_2AB dye shows minimal to no cellular toxicity at 0.5-10 μM concentration range (Figure 6a). However, in our current studies, TTPCl containing phosphonium ions showed a dose-dependent cytotoxicity with an IC_{50} value 5.4 μM and 3.3 μM in MCF-7 and MCF-10A cells, respectively (Table 2). This result indicates that TTPCl is more toxic towards non-tumorigenic cells as compared to the cancer cells. However, upon substituting TTPCl counterion with AB anion, the IC_{50} value of $[TTP]_2[AB]$ is found to be to 2.4 μM and 4.0 μM in MCF-7 and MCF-10A cells, respectively (Fig. 6(b)). These results indicate that the presence of AB counterion enhanced the chemotherapeutic activity of TTP ion towards cancerous cells. Statistical significance was determined by using a two-tailed student's t test and resulting cell viability of the nanodrug was found to be statistically significant. Thus, the ion exchange from chloride to AB complements $[TTP]_2[AB]$ NP's toxicity and selectivity towards cancerous cells than their non-tumorigenic analogue. The EPR effect also corresponds to their size-based selectivity toward cancerous cells than non-tumorigenic cells [10, 36].

[Insert Table 2]

Cellular uptake

To further investigate the internalization of NPs in cells, fluorescence emission intensity was recorded after 24 h incubation with MCF-7 cells (300 nm ex/355 nm em). Cells were washed with

PBS prior to emission measurements to remove NPs that were not internalized. A relative increase in emission intensity compared to cell media only (control) clearly indicates the internalization of both Na_2AB NPs and IL-based NPs (Figure 6d). Another experiment was performed where NPs were incubated with cell media for 30 min to investigate a potential route of uptake of the two compounds. The Na_2AB NP suspension exhibits greater emission than the control in cell media, which indicates serum in cell media may be aiding in the solvation of Na_2AB. DLS results show Na_2AB NPs sample prepared in cell media to be 7.6 nm which is much smaller than in aqueous media. It can be assumed that NPs of $[TTP]_2[AB]$ remain undissociated in cell media (no fluorescence emission compared to control) (Figure 6c). This is attributed to $[TTP]_2[AB]$ NPs superior selectivity towards cancer cells via size based EPR effect. This study is a proof of concept that by replacing a chloride ion with a fluorophore, selective toxicity of phosphonium based chemotherapeutic drug towards cancer cells can be attained. The fluorescent anion will also help to investigate the mechanism of killing of the phosphonium cation which will be published separately. A nontoxic aniline blue dye was used in this study to prove the concept of tunable cytotoxicity. In future, different fluorophores which absorb at longer wavelength will be used to perform mechanism studies due to their potential application in the market.

4. Conclusions

A simple, one-step synthesis method was used to fabricate an IL-based photosensitizing dye. The ion replacement enhanced the molar absorptivity of the dye in ethanol solvent by reducing aggregation of the molecules. NPs of $[TTP]_2[AB]$ were prepared using a facile reprecipitation method in water and these were characterized using TEM, DLS and zeta potential measurements. IL-based NPs are more stable than NPs of the parent compound. It has also been shown that the synthesized IL-based NPs exhibit 2.5 times higher cytotoxicity towards human breast cancer cells as compared to its phosphonium parent compound. These NPs are also selective towards cancerous cells. This strategy would help to design many tunable ionic liquids not only to tune the cytotoxicity only but also to investigate the mechanism of the drug.

Conflicts of Interest

The authors declare no conflict of interest.

Acknowledgments

This project was supported by the Arkansas INBRE program, with a grant from the National Institute of General Medical Sciences, (NIGMS), P20 GM103429 from the National Institutes of Health. This material is based upon work supported in part by the National Science Foundation EPSCoR Research Infrastructure under award number RII Track 4-1833004. We would also like to

acknowledge Bryan White, Qudes Al-Anbaky and Pooja Singh in Dr. Ali's research group for help with cell cultures.

References and Notes

1. DeSantis, C., Ma, J., Bryan, L., and Jemal, A. **2014**. Breast cancer statistics, 2013. *CA A Cancer Journal for Clinicians 64*, pp 52–62.

2. Partridge, A. H., Burstein, H. J., and Winer, E. P. **2001**. Side effects of chemotherapy and combined chemohormonal therapy in women with early-stage breast cancer. *Journal of the National Cancer Institute. Monographs 02115*(30), pp 135–142.

3. Carelle, N., Piotto, E., Bellanger, A., Germanaud, J., Thuillier, A., and Khayat, D. **2002**. Changing patient perceptions of the side effects of cancer chemotherapy. *Cancer* (95), pp 155–165.

4. Cuenca, A. G., Jiang, H., Hochwald, S. N., Delano, M., Cance, W. G., and Grobmyer, S. R. **2006**. Emerging implications of nanotechnology on cancer diagnostics and therapeutics. *Cancer 107*(3), pp 459–466.

5. Liu, Y., Miyoshi, H., and Nakamura, M. **2007**. Nanomedicine for drug delivery and imaging: A promising avenue for cancer therapy and diagnosis using targeted functional nanoparticles. *International Journal of Cancer 120*(12), pp 2527–2537.

6. Kasai, H., Murakami, T., Ikuta, Y., Koseki, Y., Baba, K., Oikawa, H., Nakanishi, H., Okada, M., Shoji, M., Ueda, M., Imahori, H., and Hashida, M. **2012**. Creation of Pure Nanodrugs and Their Anticancer Properties. *Angew. Chem. Int. Ed. 51*, pp 10315–10318.

7. Bae, K. H., Chung, H. J., and Park, T. G. **2011**. Nanomaterials for cancer therapy and imaging. *Molecules and Cells 31*(4), pp 295–302.

8. Onoue, S., Yamada, S., and Chan, H. K. **2014**. Nanodrugs: Pharmacokinetics and safety. *International Journal of Nanomedicine 9*(1), pp 1025–1037.

9. Zhang, J., Tang, H., Liu, Z., and Chen, B. **2017**. Effects of major parameters of nanoparticles on their physical and chemical properties and recent application of nanodrug delivery system in targeted chemotherapy. *International Journal of Nanomedicine 12*, pp 8483–8493.

10. Fang, J., Nakamura, H., and Maeda, H. **2011**. The EPR effect: Unique features of tumor blood vessels for drug delivery, factors involved, and limitations and augmentation of the effect. *Advanced Drug Delivery Reviews 63*(3), pp 136–151.

11. Liu, J., Liu, J., Huang, Y., Kumar, A., Tan, A., Jin, S., Mozhi, A., and Liang, X. **2013**. PH-Sensitive nano-systems for drug delivery in cancer therapy pH-Sensitive nano-systems for drug delivery in cancer therapy. *Biotechnology Advances 32*(4), pp 693–710.

12. Vladimir P. Torchilin. **2016**. Multifunctional, stimuli-sensitive nanoparticulate systems for drug delivery. *Nat Rev Drug Discov 176*(1), pp 139–148.

13. Mou, X., Ali, Z., Li, S., and He, N. **2015**. Applications of magnetic nanoparticles in targeted drug delivery system. *Journal of Nanoscience and Nanotechnology 15*(1), pp 54–62.

14. Parveen, S., Misra, R., and Sahoo, S. K. **2012**. Nanoparticles : a boon to drug delivery , therapeutics , diagnostics and imaging. *Nanomedicine: Nanotechnology, Biology, and Medicine 8*(2), pp 147–166.

15. Zhang, R., Xing, R., Jiao, T., Chen, C., Ma, K., Ma, G., and Yan, X. **2016**. Carrier-Free, Chemophotodynamic Dual Nanodrugs via Self-Assembly for Synergistic Antitumor Therapy. *ACS Appl. Mater. Interfaces 8*(21), pp 13262–13269.

16. Rogers, R. D., and Seddon, K. R. **2003**. Ionic Liquids - Solvents of the Future? *Science 302*(5646), pp 792–793.

17. Greaves, T. L., and Drummond, C. J. **2008**. Protic ionic liquids: Properties and applications. *Chemical Reviews 108*(1), pp 206–237.

18. Hough, W. L., Smiglak, M., Rodríguez, H., Swatloski, R. P., Spear, S. K., Daly, D. T., Pernak, J., Grisel, J. E., Carliss, R. D., Soutullo, M. D., Davis, J. H., and Rogers, R. D. **2007**. The third evolution of ionic liquids: Active pharmaceutical ingredients. *New Journal of Chemistry 31*(8), pp 1429–1436.

19. Stoimenovski, J., MacFarlane, D. R., Bica, K., and Rogers, R. D. **2010**. Crystalline vs. ionic liquid salt forms of active pharmaceutical ingredients: A position paper. *Pharmaceutical Research 27*(4), pp 521–526.

20. Stepnowski, P., Składanowski, A. C., Ludwiczak, A., and Laczyńska, E. **2004**. Evaluating the cytotoxicity of ionic liquids using human cell line HeLa. *Human & experimental toxicology 23*(11), pp 513–7.

21. Kumar, V., and Malhotra, S. V. **2009**. Study on the potential anti-cancer activity of phosphonium and ammonium-based ionic liquids. *Bioorganic & Medicinal Chemistry Letters 19*(16), pp 4643–4646.

22. Frade, R. F. M., Matias, A., Branco, L. C., Afonso, C. A. M., and Duarte, C. M. M. **2007**. Effect of ionic liquids on human colon carcinoma HT-29 and CaCo-2 cell lines. *Green Chemistry 9*(8), pp 873–877.

23. Frade, R. F., and Afonso, C. A. **2010**. Impact of ionic liquids in environment and humans: an overview. *Human & experimental toxicology 29*(12), pp 1038–54.

24. Ranke, J., Mölter, K., Stock, F., Bottin-Weber, U., Poczobutt, J., Hoffmann, J., Ondruschka, B., Filser, J., and Jastorff, B. **2004**. Biological effects of imidazolium ionic liquids with varying chain lengths in acute Vibrio fischeri and WST-1 cell viability assays. *Ecotoxicology and Environmental Safety 58*(3), pp 396–404.

25. Dong, R., Zhong, Z., and Hao, J. **2012**. Self-assembly of onion-like vesicles induced by charge and rheological properties in anionic-nonionic surfactant solutions. *Soft Matter 8*(30), pp 7812–7821.

26. Tan, X., Zhang, J., Luo, T., Sang, X., Liu, C., Zhang, B., Peng, L., Li, W., and Han, B. **2016**. Micellization of long-chain ionic liquids in deep eutectic solvents. *Soft Matter 12*(24), pp 5297–5303.

27. Sun, P., Lu, F., Wu, A., Shi, L., and Zheng, L. **2017**. Spontaneous wormlike micelles formed in a single-tailed zwitterionic surface-active ionic liquid aqueous solution. *Soft Matter 13*(13), pp 2543–2548.

28. Ferraz, R., Costa-rodrigues, J., Fernandes, M. H., Santos, M. M., Marrucho, I. M., Rebelo, P. N., and Prudþncio, C. **2015**. Antitumor Activity of Ionic Liquids Based on Ampicillin. *ChemMed 10*, pp 1480–1483.

29. Kilaparty, S. P., Agarwal, R., Singh, P., Kannan, K., and Ali, N. **2016**. Endoplasmic reticulum stress-induced apoptosis accompanies enhanced expression of multiple inositol polyphosphate phosphatase 1 (Minpp1): a possible role for Minpp1 in cellular stress response. *Cell Stress and Chaperones 21*(4), pp 593–608.

30. Agrawal, Y., and Patel, V. **2011**. Nanosuspension: An approach to enhance solubility of drugs. *Journal of Advanced Pharmaceutical Technology & Research 2*(2), pp 81.

31. Zhang, Y., Yang, M., Portney, N. G., Cui, D., Budak, G., Ozbay, E., Ozkan, M., and Ozkan, C. S. **2008**. Zeta potential: A surface electrical characteristic to probe the interaction of nanoparticles with normal and cancer human breast epithelial cells. *Biomedical Microdevices 10*(2), pp 321–328.

32. Chen, B., Le, W., Wang, Y., Li, Z., Wang, D., Ren, L., Lin, L., Cui, S., Hu, J. J., Hu, Y., Yang, P., Ewing, R. C., Shi, D., and Cui, Z. **2016**. Targeting negative surface charges of cancer cells by multifunctional nanoprobes. *Theranostics 6*(11), pp 1887–1898.

33. Siraj, N., Kolic, P. E., Regmi, B. P., and Warner, I. M. **2015**. Strategy for Tuning the Photophysical Properties of Photosensitizers for Use in Photodynamic Therapy. *Chemistry - A European Journal 21*(41), pp 14440–14446.

34. Virkki, K., Tervola, E., Medel, M., Torres, T., and Tkachenko, N. V. **2018**. Effect of Co-Adsorbate and Hole Transporting Layer on the Photoinduced Charge Separation at the TiO2-Phthalocyanine Interface. *ACS Omega 3*(5), pp 4947–4958.

35. Förster, T., and Kasper, K. **1955**. Ein Konzentrationsumschlag der Fluoreszenz des Pyrens. *Berichte der Bunsengesellschaft für physikalische Chemie 59*(10), pp 976–980.

36. Kruger, C. A., and Abrahamse, H. **2018**. Utilisation of targeted nanoparticle photosensitiser drug delivery systems for the enhancement of photodynamic therapy. *Molecules 23*(10).

Figures

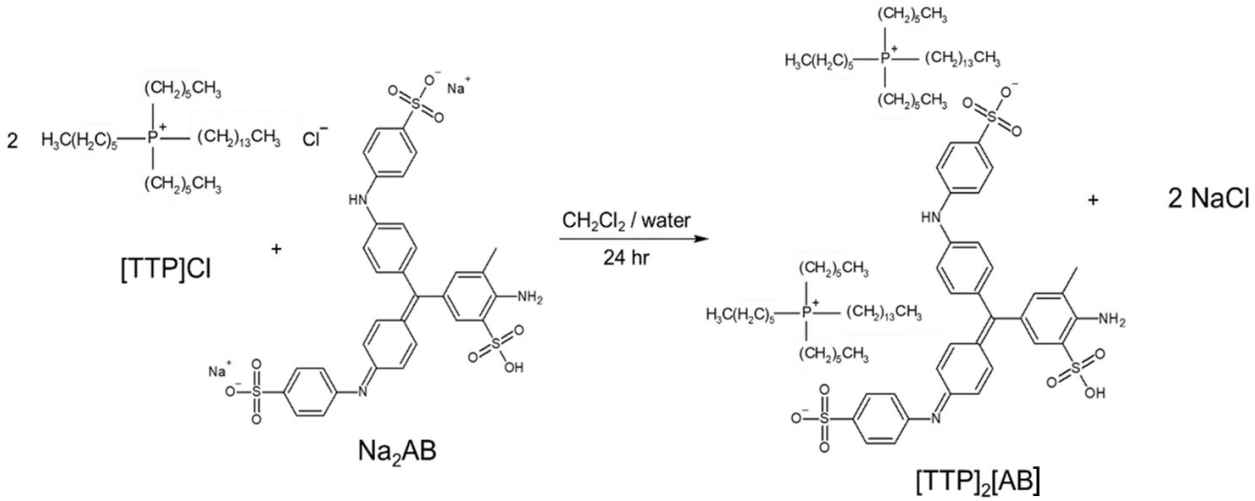

Figure 1. Synthetic route of $[TTP]_2[AB]$ via single-step ion-exchange reaction.

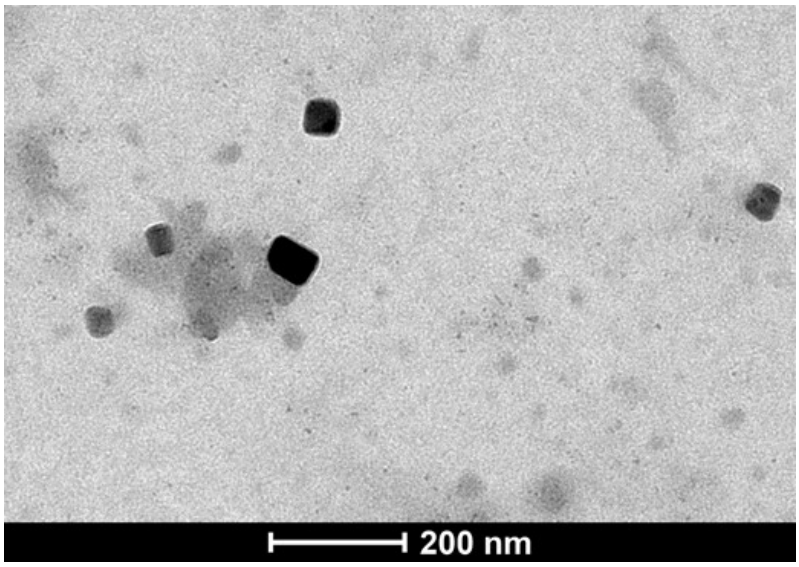

Figure 2. TEM image of $[TTP]_2[AB]$ NPs.

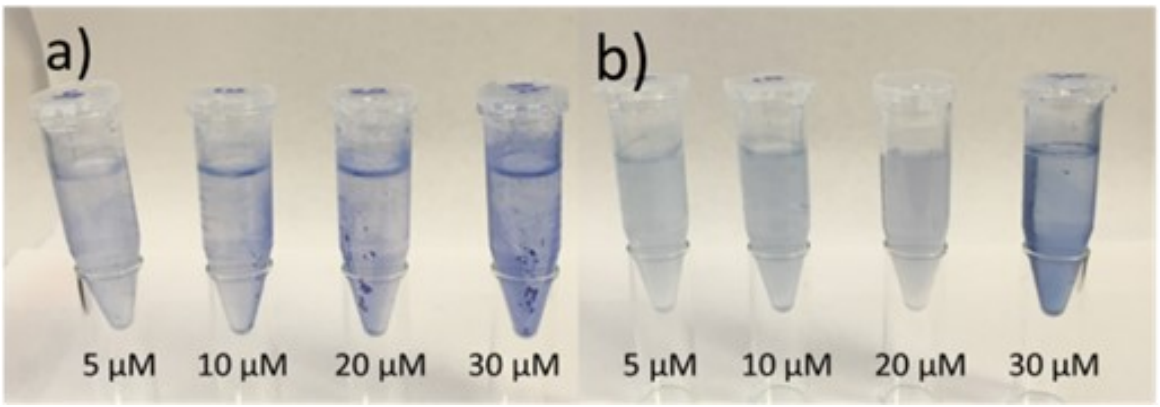

Figure 3. Various concentrations of NPs were allowed to settle in transparent tubes in the dark for 24 h in order to visually inspect the stability of the particles (precipitation/aggregation) in solution; a) Na_2AB NPs and b) $[TTP]_2[AB]$ NPs.

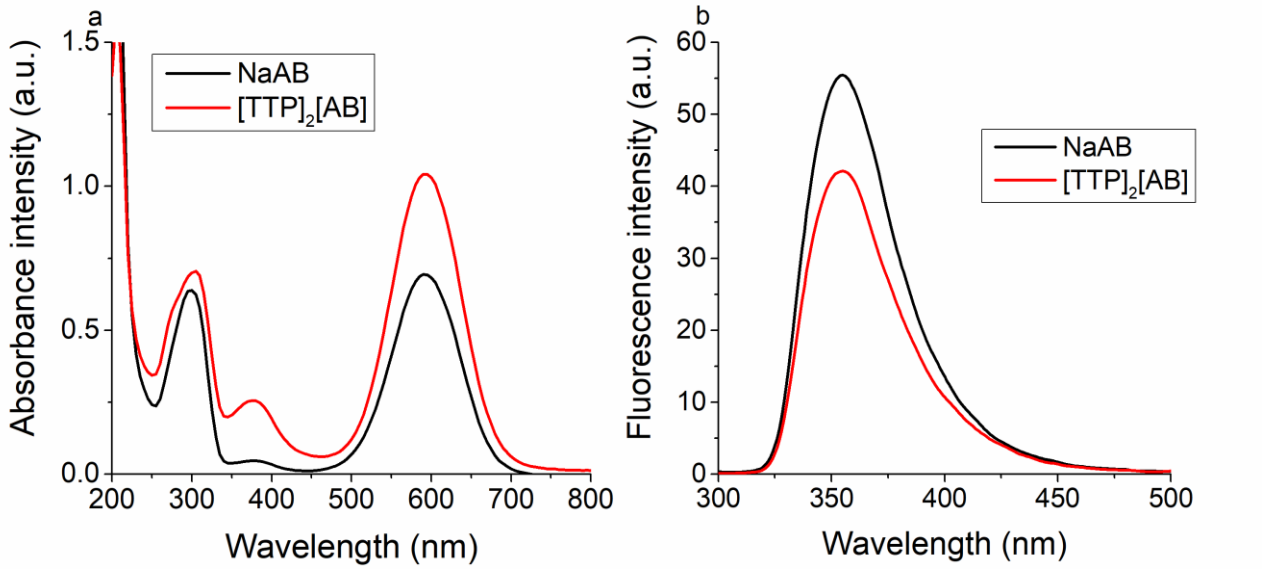

Figure 4. a) Absorbance spectra for parent compound and IL based photosensitizing dye at 20 µM in ethanol solvent and b) fluorescence spectra for both compounds at 5 µM in ethanol solvent at 290 nm excitation with 2 nm slit width.

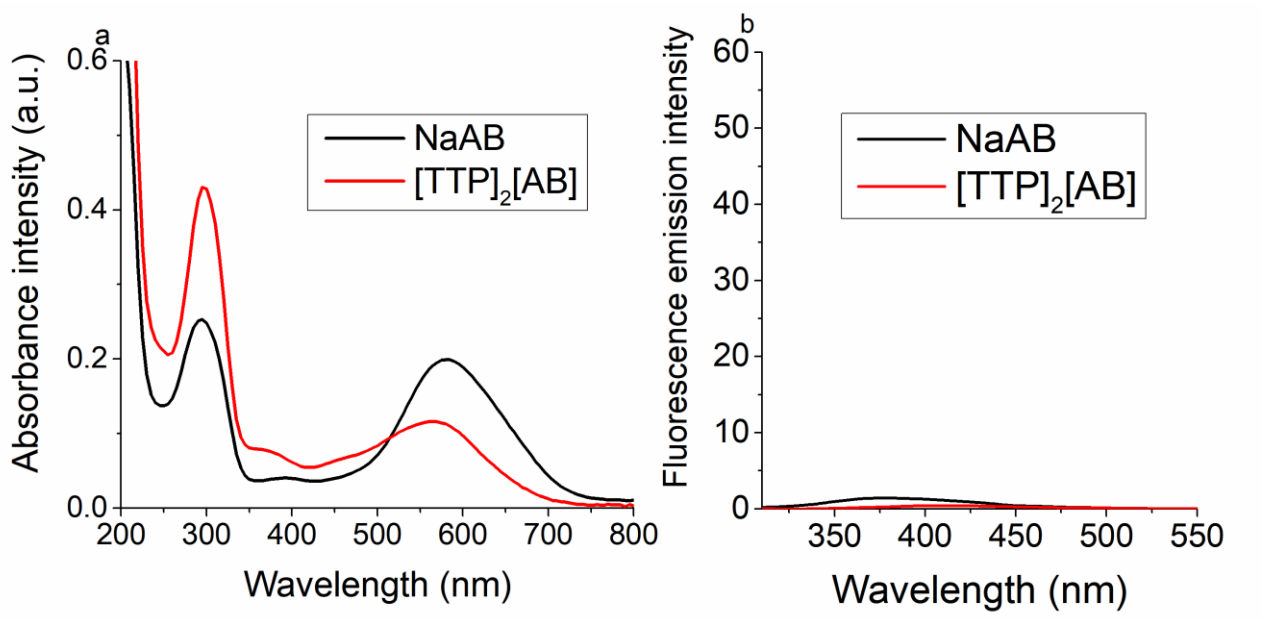

Figure 5. a) Absorbance spectra of parent photosensitizing dye and IL-based photosensitizing dye nanomaterials at 10 μM in deionized water and b) fluorescence quenching of both compounds at 5 μM in water at 290 nm excitation with 2 nm slit width.

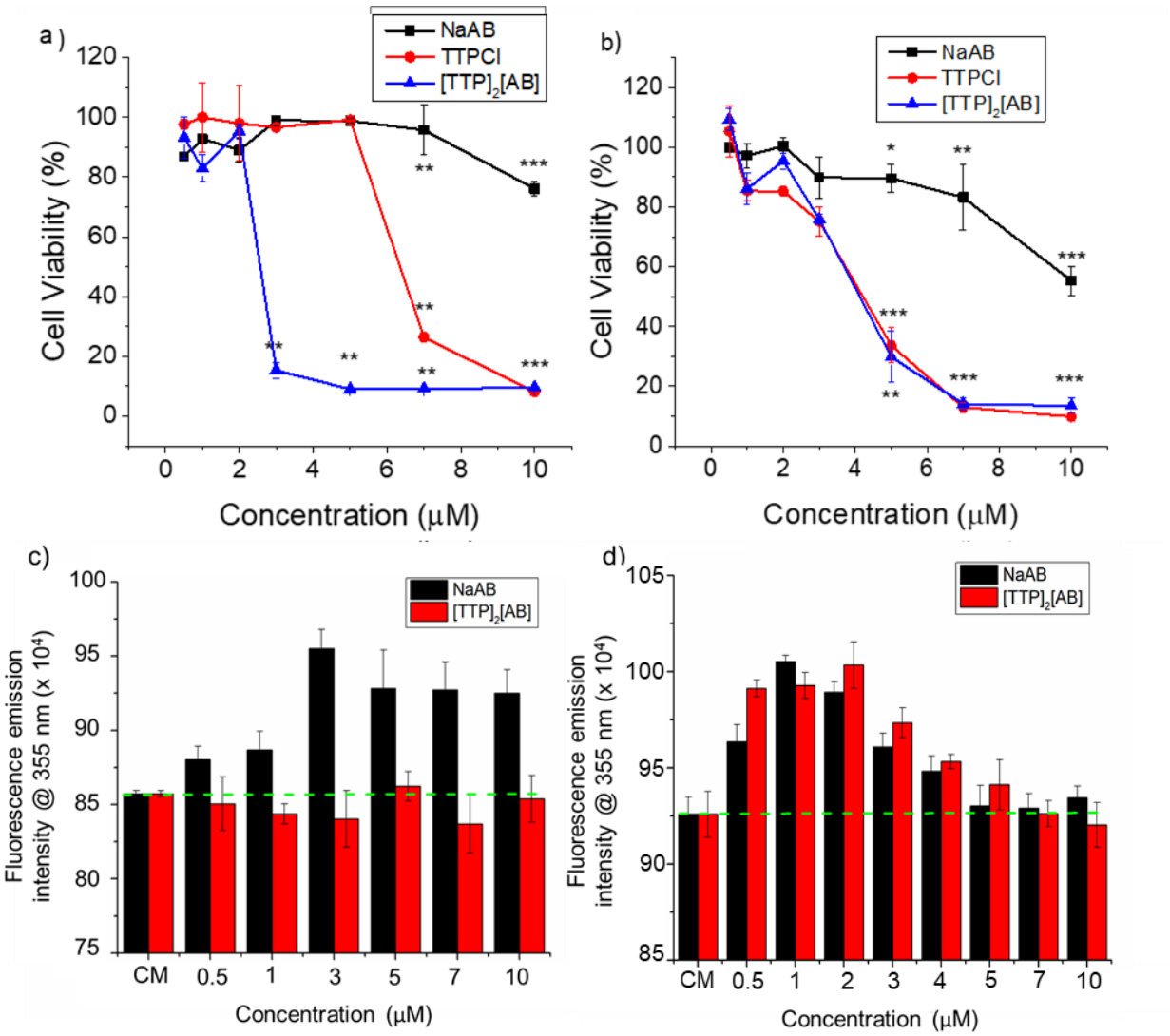

Figure 6. Cell viability of Na_2AB, TTPCl, and $[TTP]_2[AB]$ for 24 h at different concentrations in a) MCF-7 breast cancer cells and in b) MCF-10A non-cancerous cells. P values were determined using two-tailed Student's t-test and are denoted as: * $p<0.05$, ** $p<0.01$, *** $p<0.005$. c) Fluorescence emission (Ex=300 nm, Em= 355 nm) of Na_2AB and $[TTP]_2[AB]$ NPs incubated with cell media immediately (with phenol red control). d) Fluorescence emission (Ex= 300 nm, Em=355 nm) of Na_2AB and $[TTP]_2[AB]$ NPs in MCF-7 cells after 24 h incubation and washing with PBS.

Tables

Table 1. Molar extinction coefficient values for parent and IL compounds at various wavelengths in ethanol solvent and reprecipitated in water.

Compound	λ_{max} (nm) [$\varepsilon \times 10^{-4}$ (L $mol^{-1}cm^{-1}$)]
Na_2AB in ethanol	300 [3.21], 385 [0.23], 595 [3.34]
$[TTP]_2[AB]$ in ethanol	305 [3.46], 380 [1.24], 590 [6.05]
Na_2AB NPs in water	300 [3.39], 585 [3.00]
$[TTP]_2[AB]$ NPs in water	300 [5.72], 525 [1.17]

Table 2. IC_{50} values for various drug samples (μM) at a seeding density of 3×10^4 cells per well for both MCF-7 and MCF-10A cell lines. IC_{50} values were determined from dose-dependent cell viability experiments based on MTT assays.

Sample	MCF-7	MCF-10A
Na_2AB	22.18±0.63	14.01±0.39
TTPCl	5.42±0.96	3.88±0.12
$[TTP]_2[AB]$	2.41±0.14	4.00±0.77